2.6 COSMIC GPS RADIO OCCULTATION: NEURAL NETWORKS FOR TROPOSPHERIC PROFILING OVER THE INTERTROPICAL OCEAN AREA

Fabrizio Pelliccia *, Stefania Bonafoni, Patrizia Basili
University of Perugia, Perugia, Italy

Nazzareno Pierdicca
University "La Sapienza", Roma, Italy

Vittorio De Cosmo
Italian Space Agency, Roma, Italy

Piero Ciotti
University of L'Aquila, L'Aquila, Italy

1. INTRODUCTION

Global Positioning System (GPS) radio-occultation (RO) is provided as a global sounding technique for obtaining atmospheric profiles by integrating them in global models for numerical weather prediction and for climate change studies. The radio occultation system employs GPS receivers placed on a Low-Earth Orbit (LEO) satellite to sound the Earth's troposphere and ionosphere evaluating the additional delay affecting a radio signal when passing through the atmosphere due to the refractivity index magnitude and its variations (Gorbunov and Sokolovskiy 1993; Rius et al. 1998). GPS radio-occultations probe the atmosphere operating under all-weather conditions because the GPS signal wavelength do not scatter by clouds, aerosols, and precipitation, preserving a relatively high vertical resolution throughout the depth of the atmosphere associated with the limb-viewing geometry. This technique is limited by the horizontal resolution due to the Fresnel diffraction-limited pencil-shaped sampling volume of each measurement: each one has a horizontal resolution of about 200 km in the direction along the occulted link and a resolution of 1 km or better in the cross-link and vertical directions (Kursinski et al. 1997).
In this paper we have proposed a retrieval method based on neural networks to achieve atmospheric profiles from RO in wet conditions without using temperature profile at each GPS occultation from independent observations (i.e. radiosoundings or ECMWF data). We have trained three neural networks with inputs consisting of refractivity profiles computed from the occultation parameters observed by the COSMIC (Constellation Observing System for Meteorology Ionosphere and Climate) Microsat Constellation satellites provided by the COSMIC Data Analysis and Archive Center (CDAAC) of Boulder (Colorado). The network outputs are the dry and wet refractivity profiles together with the dry pressure profiles obtained from the contemporary European Centre for Medium-Range Weather Forecast (ECMWF) analysis data. We have performed the neural network training and the following independent test over the entire ocean area between Tropics by using data on summer 2006, from July 17 to August 18. The output decomposition of the refractivity components together with the estimation of the dry pressure allow to retrieve temperature and pressure of water vapor eluding the necessity to know the temperature profile from independent sources of information.

* *Corresponding author address:* Fabrizio Pelliccia, Univ. of Perugia, Dept. of Electronic and Information Engineering, via G. Duranti 93, 06125 Perugia, Italy; email: fabrizio.pelliccia@diei.unipg.it

2. NEURAL NETWORK: INPUT AND TARGET RETRIEVAL

GPS radio signals passing through the atmosphere are refracted due to the vertical refractive profile: the overall effect of the atmosphere can be characterized by a total bending angle α, an asymptotic impact parameter a and a tangent radius r_p (Kursinski et al. 1997).
By considering the assumption of local spherical symmetry, the refraction index profile n can be retrieved from measurements of α as a function of a during an occultation by using an Abel transformation as in (Fjeldbo et al. 1971):

$$n(r_p) = exp\left(\frac{1}{\pi}\int_{a_{r_p}}^{\infty}\frac{\alpha(a)}{\sqrt{a^2 - a_{r_p}^2}}da\right) \quad (1)$$

where $a_{rp} = n(r_p)\cdot r_p$ is the impact parameter for the ray whose tangent radius is r_p. The refractivity profile used as input for the neural networks training and the successive independent test is then $N=(n\text{-}1)\cdot 10^6$.

The targets for the neural networks training and the successive validation of the neural networks outputs were obtained using geopotential, temperature, specific humidity and logarithmic surface pressure from ECMWF 91 model levels analysis profiles (ECMWF website).

From these profiles, the atmospheric refractivity N at microwave wavelength were computed by (Smith and Weintraub 1953):

$$N = 77.6\frac{P_d}{T} + 72\frac{P_w}{T} + 3.75\cdot 10^5\frac{P_w}{T^2} \quad (2)$$

where P_d is the pressure of dry air in mbar, P_w the partial pressure of water vapor in mbar, T is the atmospheric temperature in Kelvin. To obtain T, P_d and P_w profiles given N, the additional constraints of ideal gas and hydrostatic equilibrium laws are required, respectively as:

$$\rho = \frac{P_d}{T}\frac{M_d}{R_0} + \frac{P_w}{T}\frac{(M_w - M_d)}{R_0} \quad (3)$$

$$dP(r) = -g\rho(r)dr \quad (4)$$

where $\rho(r)$ is the air density in kg m^{-3}, $P=P_d+P_w$, M_d and M_w are respectively the mean molecular mass of dry air and water vapor, R_0 is the universal gas constant, g the gravitation acceleration. Given N, we have a system of three equations and four unknowns (T, P_d, P_w and ρ) and therefore it is necessary to have an independent knowledge of one of the four parameters, usually the temperature, to solve the atmospheric profiling problem (Kursinski et al. 1997; Kursinski and Hajj 2001; Vespe et al. 2002).

2.1 *Selection Of COSMIC GPS Radio Occultation And Corresponding ECMWF Data*

In this paper, we have collected 1041 COSMIC GPS RO events provided by CDAAC (COSMIC website), covering the inter-tropical ocean area from July 17 to August 18, 2006. The COSMIC GPS RO and the corresponding ECMWF observations above the ocean area have been selected on the basis of the land/sea flag included in the ECMWF data, and co-located by considering a maximal interval of 1 hour and a maximal geographical coordinate distance of 0.5° between the terrestrial coordinates of the occultation points[1] and those provided in ECMWF data.

3. NEURAL NETWORK: ATMOSPHERIC PROFILING

We have designed three neural networks to solve the atmospheric profiling problem from GPS RO overcoming the constraint of temperature profile availability at each GPS occultation: the neural network predictors are the refractivity profiles $N(r)$ provided by the RO technique using (1) and the targets are the corresponding dry $N_d(r)$ and wet $N_w(r)$ refractivity profiles and the dry pressure profiles $P_d(r)$ computed from ECMWF data. $N_d(r)$ and $N_w(r)$ are respectively the first and second terms on the right-hand side of (2).

We have performed the neural network training and the following independent test over the entire ocean area between Tropics by using the available data set of 1041 refractivity profiles on summer 2006, choosing randomly, 937 profiles for the training and the remaining 104 for the independent test of the network, that represent 90% and 10% of the entire available dataset respectively. Since each profile has 689 fixed altitude levels, representing the atmosphere from 0.9 to 20 km, we have pre-processed the input and target features using Principal Component Analysis (PCA) by expanding the 689-level refractivity profiles on a basis of empirical orthogonal functions called principal components (Smith and Woolf 1976). By using the PCA technique we have reduced the number of descriptive profile parameters by exploiting the correlation among values at different altitudes. We have used only 22 principal components for the total refractivity instead of the original 689 levels, representative of the 99.9% of the total variance of the original data (Demuth et al. 2008). Concerning the neural network targets, the number of components for dry refractivity, wet refractivity and dry pressure profiles are 17, 20 and 10, respectively.

We have considered the profile data set starting from 0.9 km above the Earth surface since approximately only the 50% of the GPS occultations reaches lower levels.

[1] The occultation point is defined as the point on the Earth's surface to which the retrieved refractivity profile is assigned, located under the perigee point of the bended ray (Kuo et al. 2004)

3.1 *Early Stopping Approach*

For the training session of the neural networks, we have applied the early stopping technique, useful for determining the optimal number of training epochs. Then we have divided the training data set (937 events) in three subsets: the training subset used for the learning itself, the validation subset and the test subset used to improve the ability of generalization of the neural network, by assigning them randomly the 70% (655 events), the 15% (141 events) and the 15% (141 events) of the whole data set, respectively.
The considered feed-forward neural networks have been chosen among the possible combinations on the basis that they exhibit the lower root mean square (RMS) error computed comparing the network outputs of the test session with the corresponding ECMWF profiles, where the test session employs the 104 refractivity profiles not used in the training phase. The best neural network topologies in terms of performance for the dry refractivity, wet refractivity and dry pressure retrieval are reported in Table 1.
The hidden layers are characterized by tan-sigmoid transfer function while the output layers by linear transfer function. Instead of the standard back-propagation, for a fast training, we used the Bayesan regularization process according to Levenberg-Marquardt algorithm for a fast training (Hagan and Menhaj 1994).

EARLY STOPPING PCA			
	INPUT	HL	OUTPUT
N Dry	22	8	17
N Wet	22	10	20
P Dry	22	5	10

Table 1: Best neural network topologies named N Dry (for dry refractivity estimation), N Wet (for wet refractivity estimation) and P Dry (for dry pressure estimation): input, HL and output columns report the number of neurons for the input, hidden layer and output, respectively

4. RESULTS

4.1 *Refractivity And Pressure Estimation By Neural Network*

As shown in Figure 1, the neural networks contribute slightly to reduce the RMS error computed between refractivity profiles N obtained using Abel transformation, that are the inputs for the training of neural networks and the corresponding ECMWF N refractivity profiles, that we assume here and in the following as the true climatological variability.
Considering N estimated by the neural networks, i.e. the autotest result, the vertically averaged RMS error is 2.78 (N unit) while the corresponding vertically averaged RMS error of the refractivity profiles N obtained from Abel transformation is 3.58 (N unit). The mean standard deviation of the entire ECMWF database is 6.13 (N unit).
N_d, N_w and P_d retrieved as outputs of the neural networks, employing as input an independent set of 104 refractivity profiles N obtained from Abel transformation, exhibit the profiles of RMS error (continuous line) shown in Figure 2, Figure 3 and Figure 4 respectively, superimposed to the corresponding ECMWF standard deviation profiles (dashed line). The RMS error is computed comparing the network outputs with the corresponding ECMWF profiles.
The retrieved profiles using neural networks approach appear more consistent with the real state of the atmosphere with respect to the corresponding ECMWF database first guess.
The choice to train the networks with three outputs is justified by the necessity to retrieve atmospheric profiles overcoming the constraint of temperature profile availability at each GPS occultation, as required to solve the system of (2), (3), (4).
Also, we have chosen to estimate the dry pressure P_d from the network instead of solving the ideal gas and hydrostatic equilibrium laws in dry conditions since the error introduced by the neural networks is significatively lower with respect to the one exhibited after the integration of the (4).

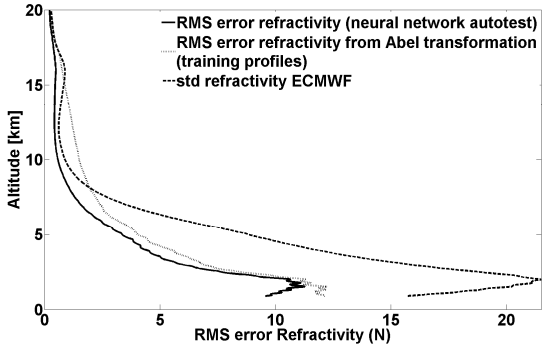

Figure 1: Neural network autotest (937 occultations): profile of RMS error for N (continuous line) obtained as output of the neural network training, profile of RMS error N from Abel transformation (dotted line) and ECMWF standard deviation profile (dashed line)

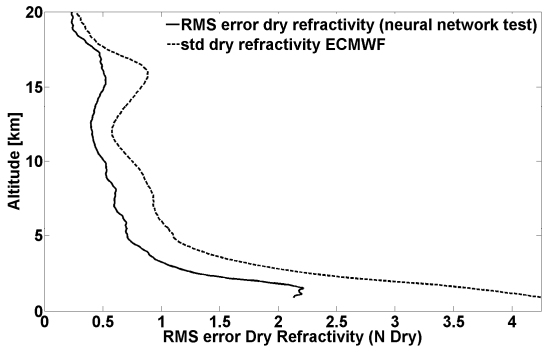

Figure 2: Neural network independent test (104 occultations): profile of RMS error for N_d (continuous line) and ECMWF standard deviation profile (dashed line)

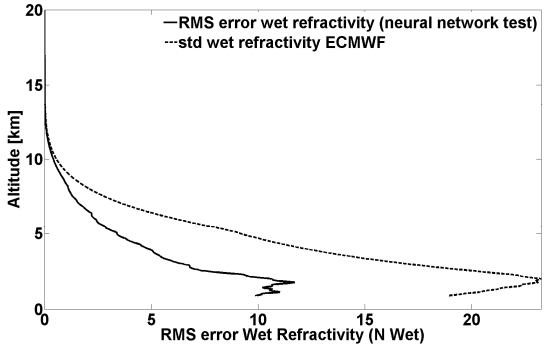

Figure 3: Neural network independent test (104 occultations): profile of RMS error for N_w (continuous line) and ECMWF standard deviation profile (dashed line)

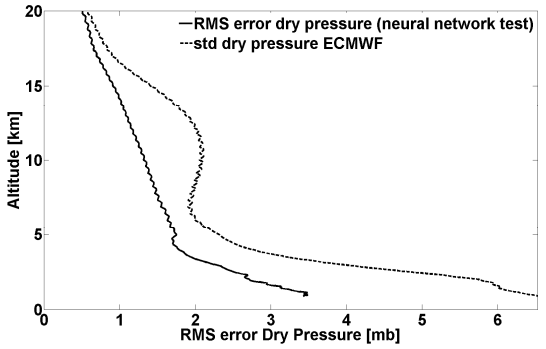

Figure 4: Neural network independent test (104 occultations): profile of RMS error for P_d (continuous line) and ECMWF standard deviation profile (dashed line)

4.2 *Temperature And Pressure Water Vapor Estimation*

With the availability of N_d, N_w and P_d, at first we can solve for temperature T in a straightforward way from the dry refractivity relation

$$N_d = 77.6\frac{P_d}{T} \quad (5)$$

and then for partial pressure water vapor P_w from the wet refractivity relation

$$N_w = 72\frac{P_w}{T} + 3.75\cdot 10^5 \frac{P_w}{T^2} \quad (6)$$

instead of solving the system of (2), (3), (4).
In Figure 5 and Figure 6 the profiles of RMS error for respectively T and P_w (continuous line) are shown superimposed to the corresponding ECMWF standard deviation profile (dashed line).
In Table 2 the averaged RMS error for the estimated profiles and the corresponding mean ECMWF standard deviation are shown.

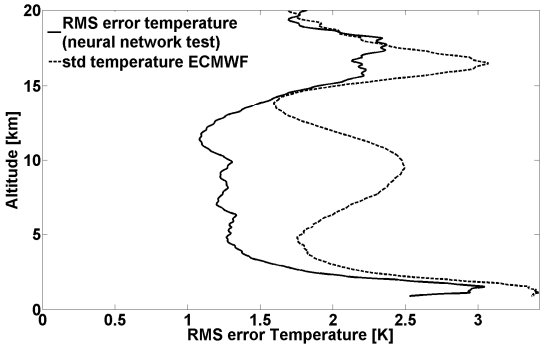

Figure 5: Neural network independent test (104 occultations): profile of RMS error for T (continuous line) and ECMWF standard deviation profile (dashed line)

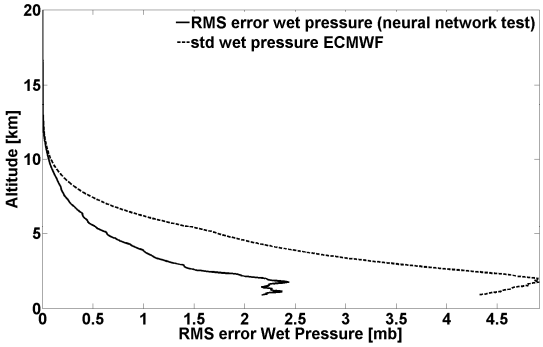

Figure 6: Neural network independent test (104 occultations): profile of RMS error for P_w (continuous line) and ECMWF standard deviation profile (dashed line)

	Vertically Averaged RMS error	Mean Standard Deviation ECMWF
Dry Refractivity	0.76 N-unit	1.21 N-unit
Wet Refractivity	2.73 N-unit	6.34 N-unit
Dry Pressure	1.61 mbar	2.55 mbar
Wet Pressure	0.54 mbar	1.27 mbar
Temperature	1.53 K	2.22 K

Table 2: Neural network independent test (104 occultations): vertically averaged RMS error for estimated profiles and corresponding mean ECMWF standard deviation

5. SUMMARY

The results have shown good performances of the neural networks using the principal component analysis for a fast and less expensive approach, exhibiting a fairly good accuracy for temperature and partial pressure of water vapor profiles.
The purpose of our analysis consists in showing the possibility to retrieve each atmospheric parameter included the wet ones only from RO refractivity, and then the ability to increase the atmospheric observations, integrating them successively in the accuracy models, thanks to a wide spatial coverage of RO soundings on the Earth. The bound of this approach is that the informative contribution brought by RO soundings is in some way connected to the necessary employment of the ECMWF atmospheric model profiles as targets for the neural network training.
The work has been sponsored by the ASI, Italian Space Agency. We wish to thank COSMIC Data Analysis and Archive Center (CDAAC) of Boulder (Colorado) for the availability of the occultation data.

REFERENCES

COSMIC website. Available via www.cosmic.ucar.edu/index.html

Demuth, H., Beale, M., Hagan, M., 2008: *Neural network toolbox for use with Matlab*, User's Guide v.6, The MathWorks

ECMWF website. Available via www.ecmwf.int

Fjeldbo, G., Kliore, A.J., Eshleman, V.R., 1971: The Neutral Atmosphere of Venus as Studied. with the Mariner V Radio Occultation Experiments. *Astron. J.*, 76, 123-140

Gorbunov, M.E., Sokolovskiy, S., 1993: Remote sensing of refractivity from space for global observations of atmospheric parameters. *Report No. 119. Max-Planck-Institut fur Meteorologie*. Hamburg

Hagan, M., Menhaj, M., 1994: Training feed-forward networks with the Marquardt algorithm. *IEEE Transactions on Neural Networks*, Vol. 5, No. 6, pp 989-993

Kuo, Y.H., Wee, T.K., Sokolovskiy, S., Rocken, C., Schreiner, W., Hunt, D., Anthes, R.A., 2004: Inversion and error estimation of GPS Radio Occultation data. *J. Meteorological Society of Japan*, Vol.82, N0. 1B, pp 507-531

Kursinski, E.R., Hajj, G.A., Schofield, J.T., Linfield, R.P., Hardy, K.R., 1997: Observing Earth's atmosphere with radio occultation measurements using the Global Positioning System. *J. Geophys. Res.*, vol. 102, N0 D19, pp. 429–465

Kursinski, E.R., Hajj, G.A., 2001: A comparison of water vapour derived from GPS occultations and global weather analyses. *J. Geophys. Res.*, vol. 106, N0 D1, pp. 1113–1138

Rius, A., Ruffini, G., Romeo, A., 1998: Analysis of ionospheric electron density distribution from GPS/MET occultations. *IEEE Trans. Geosci. Remote Sensing*, 36(2), 383-394

Smith, E.K., Weintraub, S., 1953: The constants in the equation for atmospheric refractive index at radio frequencies. *Proc. IRE*, vol.41, pp. 1035-1037

Smith, W.L., Woolf, H.M., 1976: The use of eigenvectors of statistical covariance matrices for interpreting satellite sounding radiometer observations. *J. Atmos. Sci.*, vol. 33, pp. 1127-1140

Vespe, F., Benedetto, C., Pacione, R., 2002: Water Vapor Retrieved by GNSS Radio Occultation Technique with no External Information?. *Radio Occultation Science Workshop*, Boulder, Colorado